Activator of G Protein Signaling 8 (AGS8) Is Required for Hypoxia-induced Apoptosis of Cardiomyocytes
ROLE OF G$\beta\gamma$ AND CONNEXIN 43 (CX43)*[S]

Motohiko Sato[‡1,2], **Qibin Jiao**[‡1], **Takashi Honda**[‡], **Reiko Kurotani**[‡], **Eiji Toyota**[§], **Satoshi Okumura**[‡], **Tatsuo Takeya**[¶], **Susumu Minamisawa**[‖], **Stephen M. Lanier**[**], and **Yoshihiro Ishikawa**[‡3]

From the [‡]Cardiovascular Research Institute, Yokohama City University School of Medicine, Fukuura, Yokohama 236-0004, Japan, the [§]Department of of Cardiology, Kawasaki Medical School, Kurashiki 701-0192, Japan, the [¶]Graduate School of Biological Sciences, Nara Institute of Science and Technology, Nara 630-0101, Japan, the [‖]Department of Life Science and Medical Bioscience, Waseda University, Tokyo 162-8480, Japan, and the [**]Department of Pharmacology, Medical University of South Carolina, Charleston, South Carolina 29425

Ischemic injury of the heart is associated with activation of multiple signal transduction systems including the heterotrimeric G-protein system. Here, we report a role of the ischemia-inducible regulator of G$\beta\gamma$ subunit, AGS8, in survival of cardiomyocytes under hypoxia. Cultured rat neonatal cardiomyocytes (NCM) were exposed to hypoxia or hypoxia/reoxygenation following transfection of AGS8siRNA or pcDNA::AGS8. Hypoxia-induced apoptosis of NCM was completely blocked by AGS8siRNA, whereas overexpression of AGS8 increased apoptosis. AGS8 formed complexes with G-proteins and channel protein connexin 43 (CX43), which regulates the permeability of small molecules under hypoxic stress. AGS8 initiated CX43 phosphorylation in a G$\beta\gamma$-dependent manner by providing a scaffold composed of G$\beta\gamma$ and CX43. AGS8siRNA blocked internalization of CX43 following exposure of NCM to repetitive hypoxia; however it did not influence epidermal growth factor-mediated internalization of CX43. The decreased dye flux through CX43 that occurred with hypoxic stress was also prevented by AGS8siRNA. Interestingly, the G$\beta\gamma$ inhibitor Gallein mimicked the effect of AGS8 knockdown on both the CX43 internalization and the changes in cell permeability elicited by hypoxic stress. These data indicate that AGS8 is required for hypoxia-induced apoptosis of NCM, and that AGS8-G$\beta\gamma$ signal input increased the sensitivity of cells to hypoxic stress by influencing CX43 regulation and associated cell permeability. Under hypoxic stress, this unrecognized response program plays a critical role in the fate of NCM.

G-protein-coupled receptors (GPCRs)[4] are signaling proteins on the cell surface responsible for mediating various ligands, such as hormones and neurotransmitters. Activation of cell surface GPCRs initiates nucleotide exchange on Gα subunits, which leads to a conformational change of G$\alpha\beta\gamma$ and subsequent transduction of signals to various intracellular effector molecules (1–3). In addition to such established signaling pathways, recent studies indicate the existence of a novel class of regulatory proteins for heterotrimeric G-proteins. These regulatory proteins may provide alternative signal processing via G$\alpha\beta\gamma$, Gα, or G$\beta\gamma$ subunits distinct from typical GPCR pathways, and identifying these mechanisms may uncover unrecognized roles of G-proteins beyond simple transducers of signals from GPCRs (4–6).

During the alteration of signaling pathways in disease states, such regulatory proteins may be involved in adaptation programs of cells to maintain homeostasis (7–11). Genetic modification of regulatory proteins for G-proteins leads to the development of cardiovascular dysfunction in mice including hypertension, maladaptive response to pressure overload, or altered baroreceptor reflex (9, 12, 13). Thus, such regulatory accessory proteins may be involved in the development of disease via either regulating GPCR-initiated signals or by undefined, alternative G-protein signaling pathways operating independent of the receptor.

In our efforts to adaptation-specific signal regulators for G-protein systems, we identified a novel receptor-independent G-protein activator, activator of G-protein signaling 8 (AGS8), from a cDNA library of rat hearts subjected to repetitive transient ischemia with the development of collateral vessels (8). Initial observations indicated that AGS8 was up-regulated in cardiomyocytes in response to transient ischemia and hypoxia.

FIGURE 1. **The schematic diagram of AGS8 and the characterization of AGS8siRNA or AGS8 antibodies.** *A*, schematic diagram of AGS8 showing target regions of siRNAs and epitopes of antibodies. *Arrowheads* indicate the target for each siRNA for AGS8. *Solid bars* indicate the epitope of each AGS8 antibodies. AGS8-C, 372 amino acid of the C-terminal region of AGS8. *B*, suppression of AGS8 by siRNA in cultured cardiomyocytes. Neonatal cardiomyocytes were transfected with 50 nm siRNAs for AGS8 as well as control siRNAs. Control siRNA is the universal negative siRNA control designed to minimize sequence homology to any known vertebrate transcript (Stealth RNAi Negative Control). 48 h after transfection, the level of mRNA of AGS8 was analyzed by real-time PCR. Transfection efficiency of siRNA was estimated 70–80% using FITC-labeled dsRNA (Block It Fluorescent Oligo, Invitrogen) (*right panel*). *, $p < 0.05$ *versus* negative siRNA. $n = 8$ from four independent experiments. *C*, detection of expressed AGS8 by AGS antibody (TA829). COS7 cells were transfected with pcDNAHis (4 μg/35-mm dish) or pcDNAHis::AGS8 (4 μg/35-mm dish). After 48 h of transfection, cells were solubilized into Laemmli buffer, and 10 μg of cell lysates were subjected to immunoblot. (TA829, 1:1000; TB087101, 1:3000). *D*, immunofluorescence stain of expressed AGS8 in COS7 cells. COS7 cells transfected with pcDNA::AGS8 (4 μg/35-mm dish) were subjected to immunofluorescence stain for AGS8 (TA829, 1:200, *red*, *arrow*) and nuclei (DAPI, *blue*). *E*, immunoprecipitation of AGS8 from cell lysate. 3 μg of AGS8 antibody (TA829) or rabbit IgG was added to 1 mg of lysate prepared from COS7 cells transfected with pcDNAHis vector (12 μg/dish) or pcDNAHis::AGS8 (12 μg/dish) and incubated 18 h at 4 °C with rotation. The antibody was absorbed to protein G-Sepharose (25 μl of a 50% slurry). The pellets were eluted in 30 μl of 2× Laemmli buffer and subjected to SDS-PAGE. AGS8 was detected by AGS8 antibody (TB087101, 1:1000).

AGS8 directly interacted with G$\beta\gamma$ and regulated G$\beta\gamma$ signaling in cells (8, 14). The induction of AGS8 in tissue and cells suggests that AGS8 may be involved in the adaptation of cardiomyocytes to ischemia, which determines the survival or death of cells.

Here, we report the involvement of AGS8 in cardiomyocyte survival following exposure to hypoxic stresses, and identify protein(s) associated with AGS8 that may regulate cellular events in response to stress. The suppression of AGS8 completely blocked hypoxia-induced apoptosis of cardiomyocytes, indicating that AGS8 is required for hypoxic stress-induced cell death. AGS8 formed complexes with a channel protein connexin 43 (CX43) and regulated its phosphorylation in a G$\beta\gamma$-dependent manner. AGS8siRNA blocked hypoxia-induced internalization of CX43 from the cell-surface that was associated with the altered permeability of molecules flowing through CX43. Interestingly, such AGS8-mediated regulation of CX43 was not observed for receptor-stimulated internalization of CX43 by epidermal growth factor (EGF). Subsequent experiments indicated that the effects of AGS8siRNA were mimicked by a G$\beta\gamma$ signal inhibitor. AGS8-G$\beta\gamma$ may influence the sensitivity of cells to hypoxia via regulating the permeability of CX43

in the membrane. Such undefined regulatory mechanism may play critical roles in the survival of cardiomyocytes.

EXPERIMENTAL PROCEDURES

Materials—Anti-connexin 43 antibody, β-actin antibody, IGEPAL CA-630 were purchased from Sigma. Anti-connexin 43 monoclonal antibody and phospho-connexin 43 (Ser-368) were obtained from Chemicon and Cell Signaling Technology, respectively. Anti-desmoplakin 1&2 antibody and anti-N-cadherin antibody were purchased from PROGEN Biotechnik GmbH (Heidelberg, Germany) and BD Transduction Laboratories, respectively. Anti-Xpress antibody and Lipofectamine 2000 Reagent were purchased from Invitrogen. Anti-Gβ antibody and phospho-connexin 43 (Ser-262) were obtained from Santa Cruz Biotechnology. Rat recombinant epidermal growth factor and Gallein were purchased from Funakosi (Tokyo, Japan) and Calbiochem, respectively. PMH::connexin 43 (rat) was prepared as described previously (15).

Transfection of Small Interfering RNA (siRNA) and Plasmid to Cultured Cardiomyocytes—A double-strand siRNA oliogonucleotide to rat AGS8 (DQ256268) was synthesized (Stealth siRNA, Invitrogen) as follows: AGS8 siRNA1 (nt 320–
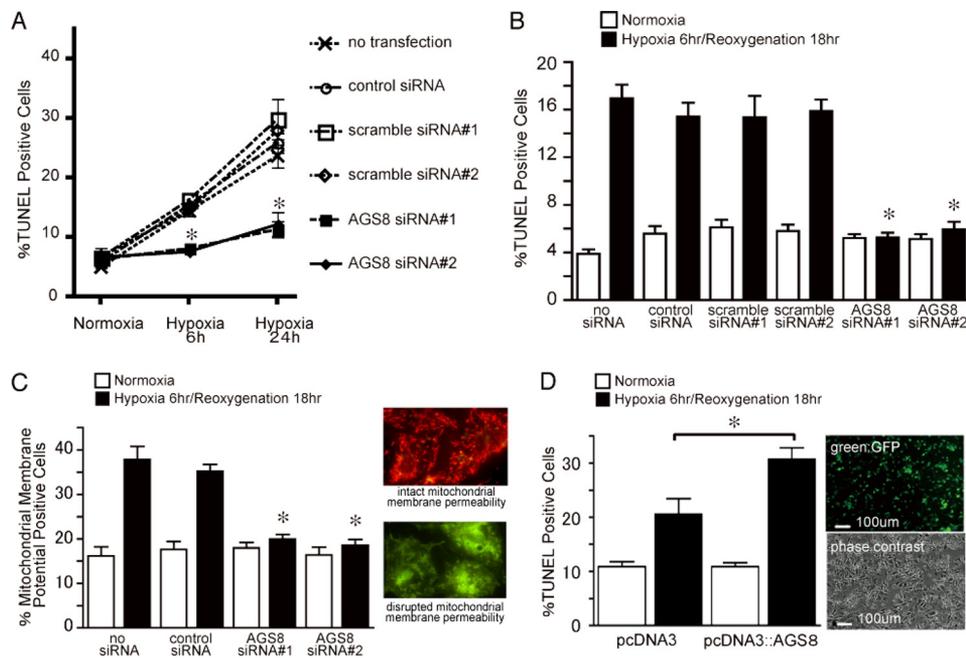
FIGURE 2. **Effect of suppression of AGS8 on apoptosis of cardiomyocytes exposed to hypoxia or hypoxia/reoxygenation.** *A*, effect of suppression of AGS8 on hypoxia-induced apoptosis of cardiomyocytes. Neonatal cardiomyocytes were exposed to hypoxia (1% oxygen) or cultured in normoxia as indicated duration following transfection of siRNA. TUNEL-positive cells were counted from 3000 cells of 10 independent fields in each experiment (magnification, 10×20). *, $p < 0.05$ *versus* scramble siRNA at the same condition; $n = 6$–7 of four independent experiments. *B*, effect of suppression of AGS8 on apoptosis of cardiomyocytes following hypoxia/reoxygenation. Neonatal cardiomyocytes were subjected to sequential exposure of 6 h of hypoxia (1% oxygen) followed by 18 h of reoxygenation 48 h after transfection of siRNA. TUNEL-positive cells were counted from 3000 cells of 10 independent fields in each experiment (magnification, 10×20). *, $p < 0.05$ *versus* scramble siRNA at the same condition. $n = 8$–12 of five independent experiments. *C*, effect of suppression of AGS8 on apoptosis following hypoxia/reoxygenation. Loss of membrane potential of mitochondria was determined utilizing fluorescence dye staining from 2000 cells of 10 independent fields in each experiment. $n = 6$–10 of five independent experiments. The *right panel* indicates the representative of fluorescence signals determined by this method. *, $p < 0.05$ *versus* scramble siRNA at the same condition. *D*, effect of overexpression of AGS8 on apoptosis of cardiomyocytes following hypoxia/reoxygenation. Neonatal cardiomyocytes were subjected to sequential exposure of 6 h of hypoxia (1% oxygen) followed by 18 h of reoxygenation following transfection of pcDNA3 or pcDNA3::AGS8. TUNEL-positive cells were counted from 3000 cells of 10 independent fields in each experiment (magnification, 10×20). Transfection efficiency was estimated at 50–60% using the GFP vector (*right panel*). *, $p < 0.05$. $n = 10$ from five independent experiments.

345, sense: 5′-CCAGAGAUGAGAGAUCGCAUGAAAU-3′), AGS8siRNA2 (nt 2048–2073, sense: 5′-UGGGUCACUUUA-GUUUGAUACGGAA-3′), scramble control from AGS8 siRNA1 (sense: 5′-CCAAGGUGAGAUAGCACGUAAG-AAU-3′), scramble control for AGS8 siRNA2 (sense: 5′-UGG-UCACGAUUGUUUCAUAGUGGAA-3′) (Fig. 1*A*). The conditions and duplex eliciting the most effective reduction in AGS8 were determined in a series of preliminary experiments. Cultured neonatal cardiomyocytes at 1.2×10^5 cell in 24-mm plates were transfected with siRNA using Lipofectamine 2000 according to the manufacturer's instructions. Briefly, RNAi 1 and 2 individually (50 nM) in 10 μl of OPTI-MEM I medium (Invitrogen) and 0.125 μl of Lipofectamine 2000 in 10 μl of OPTI-MEM I media were mixed and then added to the mixture in 24-mm dishes. The transfection efficiency of FITC-labeled oligonucleotide was 70–80% and siRNA for AGS8 did not influence the level of mRNA of β-actin in the condition used (Fig. 1*B*). Negative controls of siRNA for AGS8 were scrambled sequence of siRNA for AGS8 or universal control sequence, which has minimized homology to any known vertebrate transcript with similar GC content (Stealth RNAi Negative Control, Invitrogen). To overexpress AGS8, pcDNA3::AGS8 was trans-

ferred to cardiomyocyte utilizing viral envelope system in according to the manufacturer's instructions (GenomOne-Neo, Ishihara Corp. Osaka, Japan). The increase of mRNA of AGS8 was confirmed by real-time PCR following transfection of pcDNA3::AGS8.

Generation of AGS8 Antibody— Antipeptide AGS8 antiserum (TB087101 serum) was generated by immunizing rabbits with the synthetic peptide C-[612]STSPLSRGWK-DRQDTH-A[628] following KLH conjugation (Fig. 1*A*). Another AGS8 antiserum (TA829 serum) was generated by immunizing rabbits with a recombinant protein of AGS8 (M1-K330) synthesized as glutathione *S*-transferase (GST) fusion protein in bacteria (Fig. 1*A*). The antiserums were affinity purified and used in subsequent experiments. The antibodies for GST proteins were removed from TA829 by filtration of immune sera through immobilized GST affinity column. Antiserum was characterized by analysis of varying amounts of GST-AGS8 fusion proteins and/or extracts from COS7 cells transfected with pcDNA3::AGS8 to determine optimal conditions for immunoblotting. Purified antibodies (TA829, 0.4 mg/ml; TB087101, 1.0 mg/ml) were used for immuno-

blotting (TA829, 1:1000; TB087101, 1:1000 to 3000) (Fig. 1*C*), immunostain (TA829, 1:100–200) (Fig. 1*D*) and immunoprecipitation (TA829, 1–3.5 μg per sample) (Fig. 1*E*).

Detection of Apoptosis: In Situ Assay for Apoptosis Detection— *In situ* labeling of fragmented DNA in cardiac myocytes was detected by TACS2 TdT-Blue Label *in Situ* Apoptosis Detection kit (Travigen, Inc., Gaithersburg, MD), that detects DNA breaks in genomic DNA by enzymatic incorporation of biotinylated nucleotides followed by the binding of streptavidin-peroxidase conjugates, according to the manufacturer's instructions. Briefly, myocytes were fixed with 3.7% formaldehyde in phosphate-buffered saline for 10 min and with 70% ethanol for 5 min and then incubated in proteinase K (0.02 mg/ml) at room temperature for 5 min. The cells were incubated with 2% hydrogen peroxide for 5 min and washed with labeling buffer consisting of 50 mM Tris (pH 7.5), 5 mM $MgCl_2$, 60 μM 2-mercaptoethanesulfonic acid, and 0.05% bovine serum albumin, followed by 60 min of incubation at 37 °C in labeling buffer containing 150 μM dATP, 150 μM dGTP, 150 μM dTTP, 5 μM biotinylated dCTP, and 40 units/ml of the Klenow fragment of DNA polymerase I. Untreated myocytes incubated with or without 2 mg/ml DNase in the labeling buffer were used as positive or
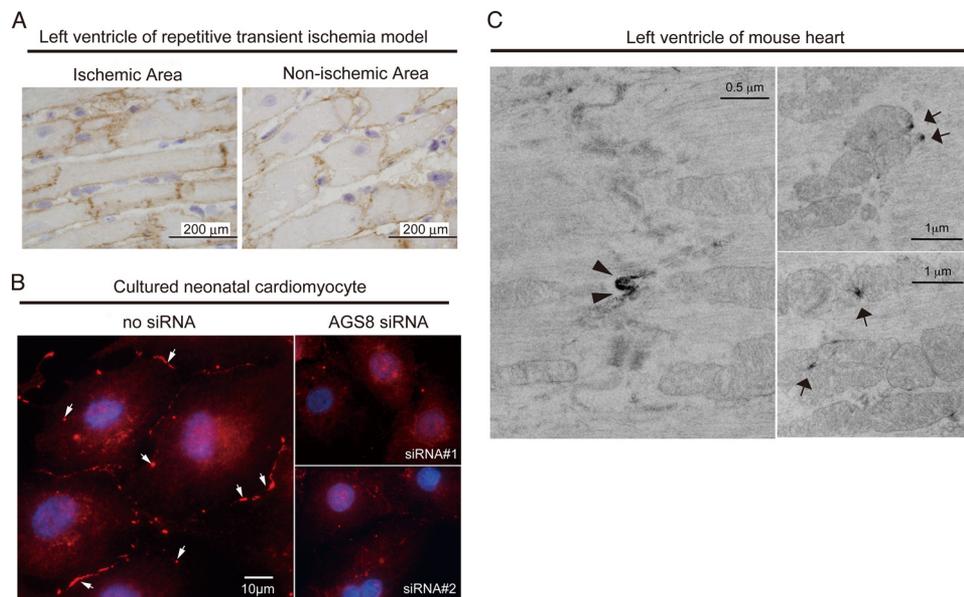
FIGURE 3. **Subcellular distribution of AGS8.** *A*, immunohistochemical staining for AGS8 (TA829, 1:200) of ischemic area (*left*) or non-ischemic area (*right*) of the left ventricle of repetitive transient ischemia model of rat prepared as described previously (8, 18). Frozen section (8 μm) of the rat heart was subjected to immunohistochemical stain as described under supplemental data. *B*, immunofluorescence stain for AGS8 (TA829, 1:200, *red*, *arrow*) and nuclei (DAPI, *blue*) of cultured neonatal cardiomyocyte. The immunoreactive signal in the plasma membrane was remarkably reduced following transfection of AGS8siRNA1 or AGS8siRNA2 (*right panels*). The data are representative of four independent experiments with similar results. *C*, analysis of subcellular localization of AGS8 by immunoelectron microscopy. The fixed mouse heart section was subjected to immunoelectron microscopy as described under supplemental data. AGS8 signals were identified in the cellular junction (*left panel*, ×18,500) as well as mitochondria (*right panels*, ×11,100).

negative controls, respectively. The incorporated biotinylated dCTP was then detected with strepavidin-peroxidase conjugate and revealed in 0.5 mg/ml diaminobenzidine for 10 min. Nuclear brown staining was viewed under a light microscope.

Assessment of Mitochondrial Membrane Potential—Loss of mitochondrial membrane potential was assessed with a fluorescence microscope (Nikon TE2000U microscope, NIKON, Tokyo, Japan) after staining with MitoCapture (BioVision, Moutain View, CA), in which cells were stained with a cationic dye that fluoresced differently in healthy *versus* apoptotic cells. Cardiomyocytes were incubated MitoCapture for 15 min at 37 °C. After the dye was applied, images were captured by fluorescence microscopy within 30 min with microscope. A 488-nm filter and 543-nm filter were used for excitation, and the resultant red and green fluorescence were quantified with
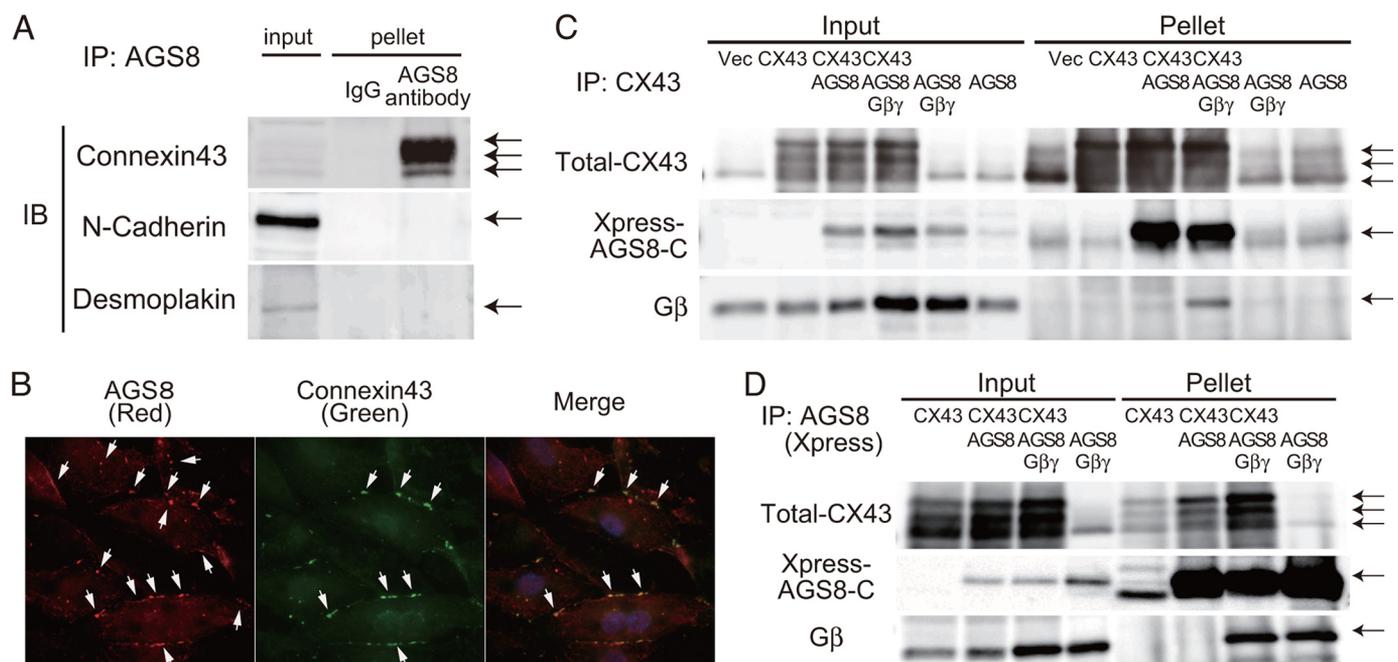
FIGURE 4. **Association of AGS8 with connexin 43.** *A*, determination of junctional proteins co-immunoprecipitated by anti-AGS8 antibody (TA829). Tissue preparation and immunoprecipitation were performed as described under supplemental data. Connexin 43 was co-immunoprecipitated by AGS8 antibody (TA829, 3.5 μg) from −1 mg of solubilized crude membrane of rat left ventricle in immunoprecipitation (IP) buffer (50 mM Tris, pH 7.4, 150 mM NaCl, 5 mM EDTA, 1% Igepal CA-630, a protease inhibitor tablet-Complete Mini (Roche Applied Science)). *B*, detection of co-localization of AGS8 with connexin 43. Cultured neonatal cardiomyocytes were fixed and stained for AGS8 (*left panel*, TA829 antibody, 1:200, *red*, *arrow*), connexin 43 (*middle panel*, mouse monoclonal connexin 43 antibody (MAB3068, CHEMICON), 1:100, *green*, *arrow*), and nuclei (DAPI, *blue*). Co-localization of connexin 43 with AGS8 (*yellow*, *arrow*) is shown in the *right panel* (*merge*). *C* and *D*, an interaction of C-terminal AGS8 (AGS8-C) with connexin 43 and/or Gβγ subunit. COS7 cells in a 100-mm dish were transfected with a combination of pcDNA3, pMH::connexin 43 (3 μg/dish), pcDNAHis::AGS8-C (6 μg/dish), pcDNA3::Gβ₁ (1.5 μg/dish), and/or pcDNA3::Gγ₂ (1.5 μg/dish). The amount of DNA transfected was adjusted to 12 μg per dish with pcDNA3 vector. The preparation of cell lysate and immunoprecipitation was performed as described under supplemental data. AGS8-C was immunoprecipitated by 1.5–2 μg of CX43 antibody (*C*) or Xpress antibody (*D*) from 500–800 μg of cell lysate in IP buffer, and the pellet was subjected to immunoblot to detect protein as indicated in the figure. The transferred membrane was reprobed with antibodies as indicated in the figure. The data are representative of five independent experiments with similar results.

GFP-B (NIKON, Tokyo, Japan) and TRITC (NIKON, Tokyo, Japan) filters, respectively. The red emission of the dye is due to a potential-dependent aggregation in the mitochondria reflecting normal membrane potential. Green fluorescence reflects the monomeric form of MitoCapture, appearing in the cytosol after mitochondrial membrane depolarization (16).

Dye Uptake Study—Cells were incubated with 1 mM Lucifer Yellow (LY) (Molecular Probes) for 30 or 45 min in normal culture medium. Unincorporated LY was removed, and cells were rinsed with phosphate-buffered saline. The fluorescence of LY was immediately evaluated by fluorescence microscopy (B-3A filter, TE2000-E, NIKON, Tokyo, Japan). The signal intensity of fluorescence of LY was quantified in 10 randomly selected fields (10 × 20) using NIS-Elements 3.0 software (NIKON, Tokyo, Japan). The non-selective binding of LY was determined by fluorescence in the presence of a connexin hemichannel blocker, 50 μM Lanthanum (Sigma-Aldrich), which was added 30 min prior to LY.

Miscellaneous Procedures and Statistical Analysis—Immunoblotting and data analysis were performed as described previously (7, 8, 17). The luminescence images captured with an image analyzer (LAS-3000, FUJIFILM, Tokyo, Japan) were quantified using Image Gauge 3.4 (FUJIFILM, Tokyo, Japan). Data are presented as mean ± S.E. from independent experiments as described in the figure legends. Statistics were performed using two-way and/or one-way ANOVA by Tukey's multiple comparison post-hoc test otherwise indicated in the text. All statistical analyses were performed with Prism 4 (GraphPad Software).

Supplemental Data—Additional information on preparation of cardiomyocytes, cell culture, detection of apoptosis, AGS8 mRNA analysis, immunochemistry, protein preparation, and immunoprecipitation assay are provided in the supplemental data.

RESULTS

The expression of AGS8 was up-regulated in the left ventricular myocardium subjected to repetitive transient ischemia, suggesting that AGS8 might be involved in adaptation processes in an ischemic myocardium (8). Such events might include the initiation of cell death or acquisition of tolerance to ischemic injury in conjunction with the development of collateral vessels (18–20). As an initial approach to identify the physiological role of AGS8 in the heart, we investigated its involvement in the survival of cardiomyocytes following hypoxic stress.

Suppression of AGS8 in Cultured Cardiomyocytes Attenuates Hypoxia-induced Apoptosis—In the first series of experiments, AGS8 level was manipulated in cultured neonatal cardiomyocytes (NCM) before exposure to hypoxia, and their survival rate was monitored. Small interfering RNA (siRNAs) for AGS8 (AGS8siRNA) targeted two distinct regions in AGS8 (Fig. 1A). The effect of AGS8siRNA and control siRNA oligonucleotides on expression of AGS8 was determined in NCM (Fig. 1B). Both AGS8siRNAs, but not their controls, successfully suppressed the level of AGS8 of cardiomyocytes to ~30% of the level of cardiomyocytes treated with negative control siRNA.
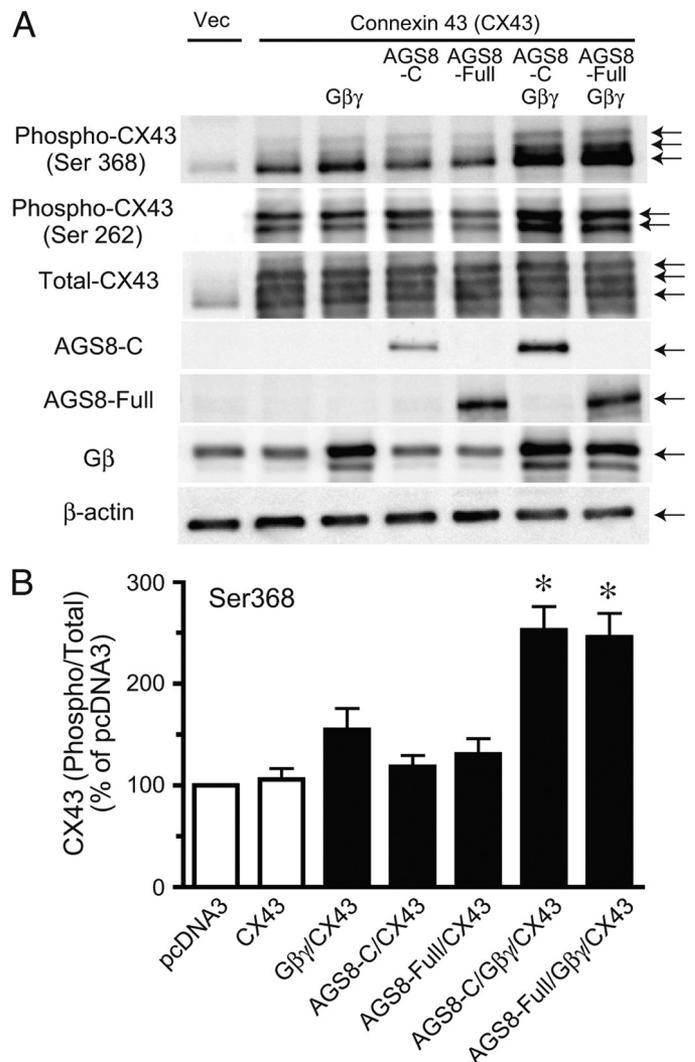
FIGURE 5. **Influence of AGS8 on phosphorylation of connexin 43 in COS7 cell.** COS7 cells in the 35-mm dish were transfected with a combination of pcDNA3, pMH::connexin 43 (1 μg/dish), pcDNAHis::AGS8-C (2 μg/dish), pcDNAHis::AGS8-full-length (2 μg/dish), pcDNA3::Gβ_1 (1 μg/dish), and/or pcDNA3::Gγ_2 (1 μg/dish) subunits. The amount of DNA transfected was adjusted to 5 μg per dish with pcDNA3 vector. After 48 h of transfection, cells were solubilized into Laemmli buffer, and 10 μg of cell lysates were subjected to SDS-PAGE. *A*, phosphorylated CX43 was detected phospho-CX43 antibody for serine 368 or serine 262. The expression of AGS8-C or AGS8-full-length was detected by Xpress antibody (1:5000) or TB087101 (1:1000), respectively. The data are representative of four independent experiments with similar results. *B*, densitometric analysis of the immunoreactive signals shown in *A*. The level of phosphorylated connexin 43 (Ser-368) was normalized with total connexin 43 and expressed as percent of pcDNA3-transfected control. *Vec*, pcDNA3; *AGS8-C*, 372 amino acids of the C-terminal region of AGS8; *AGS8-F*, full-length of AGS8. *, $p < 0.05$ *versus* connexin 43 alone. $n = 7$ from four independent experiments.

48 h after transfection with the siRNAs, NCMs were exposed to 1% O_2 hypoxia or normoxia for 6 or 24 h to induce hypoxia-mediated cell death. Hypoxic stress markedly increased the number of apoptotic cardiomyocytes and this was completely blocked by knockdown of AGS8 (Fig. 2A). Suppression of AGS8 alone did not influence the number of TUNEL-positive cells cultured in normoxic conditions throughout the experimental period[5] and control siRNA oligonucleotides were without effect.

---

[5] T. Honda, and M. Sato, unpublished observations.
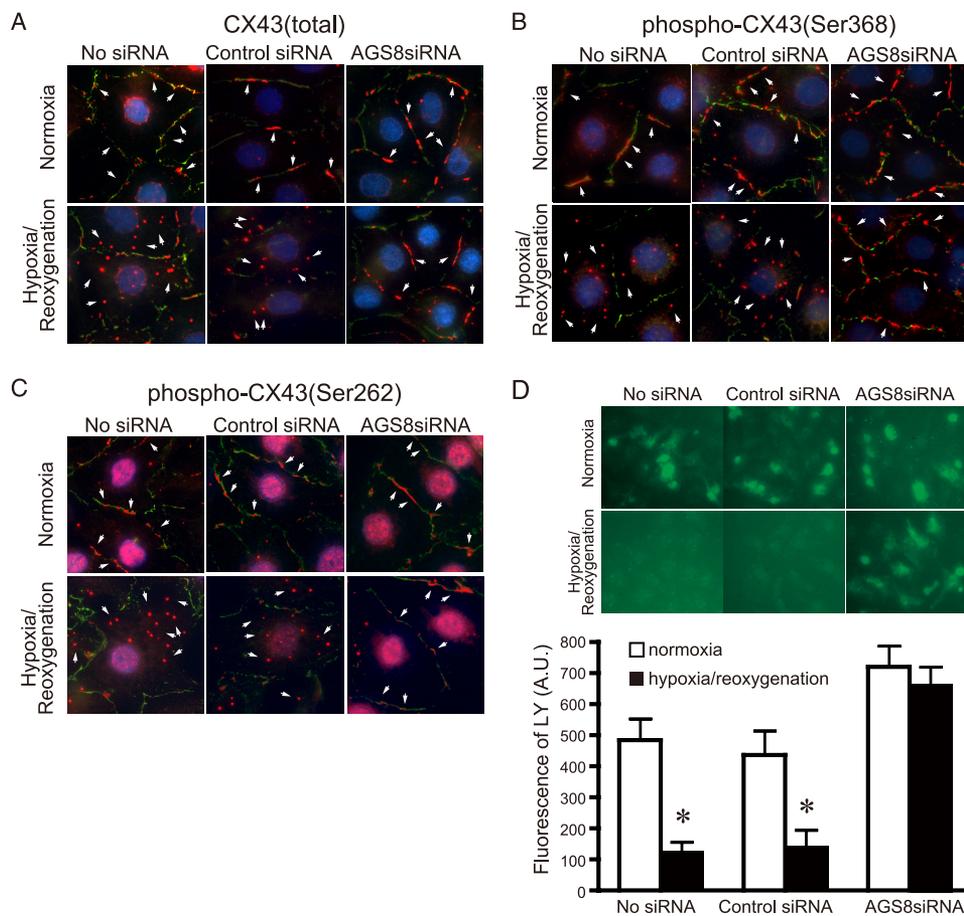
FIGURE 6. **Influence of AGS8 on hypoxia-induced internalization and the change of permeability of in cardiomyocytes.** *A–C*, an effect of AGS8siRNA on internalization of CX 43. Cardiomyocytes were exposed 3 times to 30 min of hypoxia intermittant with 30 min of reoxygenation 48 h after (without or with) transfection of universal negative siRNA control (Control siRNA) or AGS8siRNA2 (AGS8siRNA). After the third hypoxic period, cells were immediately fixed and subjected to immunofluorescence stain for total CX43 (*A*), phospho-CX43 (Ser-368) (*B*), or phospho-CX43 (Ser-262) (*C*) as described under "Experimental Procedures." For the detection of phospho-CX43, 8 μM MG132 was added to the culture prior to sequential hypoxia. The figures demonstrated the triple stain of CX43 (*red, arrow*), N-cadherin (*green*), and nuclei (DAPI, *blue*). The data are representative of 4–6 independent experiments with similar results. *D*, uptake of fluorescence dye, LY, bu the cardiomyocytes. The fluorescence of LY was evaluated by microscopy as described under "Experimental Procedures." *Upper panel*, representative pictures of cardiomyocytes incorporating LY. *Lower panel*, fluorescence of LY was quantified by the intensity of fluorescence of 10 randomly selected fields (10 $\times$ 20). *, $p < 0.05$ *versus* cells at normoxia. $n = 4$ from four independent experiments.

Suppression of AGS8 Reduced Apoptosis Induced by Hypoxia/ Reoxygenation—Reoxygenation following hypoxic periods accelerates apoptosis of cardiomyocytes (21). The influence of AGS8 on apoptosis of cardiomyocytes induced by hypoxia/reoxygenation was also examined by sequential exposure of cardiomyocytes to hypoxia (1%, O_2) for 6 h, followed by normoxia for 18 h in siRNA-transfected NCM.

Interestingly, both AGS8siRNAs blocked apoptosis of cardiomyocytes following hypoxia/reoxygenation. In this protocol, the hypoxia/reoxygenation induced apoptosis of cardiomyocytes in control groups (non-transfected control, 437 ± 29.7% increase *versus* normoxia group; Fig. 2*B*), and the number of TUNEL-positive cells was increased as compared with 6 h of straight hypoxia alone (non-transfected control, 289.8 ± 14.0% *versus* normoxia group; Fig. 2*A*).

The effect of AGS8siRNA on apoptosis was verified in another approach by detecting the change of mitochondrial membrane potential. As observed in TUNEL, AGS8siRNA

blocked the loss of membrane potential of the mitochondria (Fig. 2*C*) (22, 23).

Overexpression of AGS8 Increased Apoptosis following Hypoxia/Reoxygenation—The striking effects of AGS8siRNA on hypoxia-induced apoptosis suggested that AGS8 was required for hypoxia-mediated death of cardiomyocytes and behaved as a proapoptotic factor under hypoxic stress. However, these effects were observed by suppression of AGS8. On the other hand, AGS8 was up-regulated in the myocardium subjected to repetitive ischemia in which AGS8 was originally identified (8). Accordingly, we introduced pDNA3::AGS8 to cardiomyocytes utilizing a viral envelope system and evaluated its effect on apoptosis (Fig. 2*D*). The transfection efficiency of this procedure was ~50–60%, as estimated by fluorescence of the pEGFP vector. The number of TUNEL-positive cells increased following exposure to hypoxia (6 h)/reoxygenation (18 h) in both of cardiomyocytes transfected with pcDNA3 alone or pcDNA3::AGS8. However, the magnitude of increase in the number of TUNEL-positive cells was significantly greater in AGS8-transfected cells. Notably, the expression level of AGS8 alone did not influence the number of apoptotic cells cultured in normoxia as observed in the series of experiments with siRNAs, suggesting that the a specific function of AGS8 was revealed in response to hypoxic stress.

AGS8 was Enriched in the Plasma Membrane of Cardiomyocytes—Hypoxia-mediated cell death is involved in multiple signaling events occurring in plasma membranes and organelles in the cytosol as well as the nucleus. The ability of accessory proteins for G-proteins to influence cellular events is sometimes critically regulated by their subcellular localization or distribution (4). We next determined the localization of AGS8 in cardiomyocytes manipulating cellular events under hypoxic conditions. To address this issue, we developed an antibody against AGS8. Affinity-purified AGS8 antibody (TA829) recognized AGS8 expressed in COS7 cells by immunoblot (Fig. 1*C*). In the immunofluorescence stain, TA829 detected immunoreactive signals of AGS8 expressed in COS7 cells (Fig. 1*D*).

AGS8 antibody (TA829) recognized an immunoreactive signal in the plasma membrane of the left ventricle as well as cul-

tured cardiomyocytes (Fig. 3, *A* and *B*). Interestingly, the signals were enriched at the cell-cell interface and were attenuated in the cultured NCM following transfection of siRNAs for AGS8. The transfection of universal negative siRNA control (Stealth RNAi Negative Control) did not influence on the immunoreactive signals detected by AGS8 antibody (TA829) (supplemental Fig. S1*A*).

The localization of AGS8 in the microdomain of cells was further investigated by immunoelectronmicroscopy. AGS8 was observed in the junctional regions of plasma membrane (Fig. 3*C*, *arrowhead*) as well as the surface of mitochondria (Fig. 3*C*, *arrow*) where multiple events related to apoptosis are processed. No immunoreactive signals were detected in the absence of AGS8 antibody (supplemental Fig. S1*B*). These observations suggest that AGS8 assembles a complex with proteins in cellular junctions (24).

AGS8 Formed Protein Complexes with CX43—The possible formation of AGS8 complexes with junctional proteins was addressed by immunoprecipitation assays using the AGS8 antibody (TA829), which successfully immunoprecipitated expressed AGS8 from cell lysates (Fig. 1*E*). Interestingly, TA829 co-immunoprecipitated channel protein CX43 from rat ventricular lysate, but not other proteins typically comprising the adherence junction or desmosome, such as N-cadherin and desmoplakin, respectively (Fig. 4*A*) (24). The immunoblot of CX43 indicated enrichment of a slower migrating species upon immunoprecipitation that likely represents phosphorylated CX43 (Fig. 4*A*) (25, 26). Immunofluorescence studies also indicated co-localization of AGS8 and CX43 in cultured NCM (Fig. 4*B*). AGS8 signals were recognized in a broader area as compared with CX43, suggesting that a population of AGS8 exists apart from CX43.

Subsequent studies with transfected COS7 cells indicated that the C-terminal region of AGS8 (AGS8-C), which bound to $G\beta\gamma$, was co-immunoprecipitated by CX43 antibody (Fig. 4*C*) (8, 14). $G\beta\gamma$ also co-immunoprecipitated in the pellet with AGS8 and CX43. Conversely, CX43 was co-immunoprecipitated by Xpress antibody for AGS8-C (Fig. 4*D*). $G\beta\gamma$ was again co-immunoprecipitated with AGS8 and CX43 suggesting that $G\beta\gamma$ is involved in the assembly of the AGS8-CX43 complex.

CX43 is a transmembrane protein forming channels that pass multiple small molecules including adenosine 5′-triphosphate, adenosine, cAMP, inositol-1,4,5-trisphosphate (27–29). CX43 localized at gap junctions, plasma membranes as well as mitochondria of cardiomyocytes where AGS8 was also detected (Fig. 3) (30–32). Previous observations clearly indicated the involvement of CX43 in the ischemia/hypoxia-induced apoptosis of cardiomyocytes via alteration of cell permeability to small molecules (26, 33–36). The phosphorylation status and subcellular localization of CX43 are suggested to be critical for the apoptotic process of cells under hypoxic stress (26, 33, 34, 36).

AGS8 may regulate hypoxia-induced apoptosis via CX43 as an unexpected target of G-protein signaling. Therefore, the effects of AGS8 on the regulation of CX43 were addressed by determining the impact of altered AGS8 expression in cardiomyocytes on CX43 phosphorylation, CX43 subcellular dis-
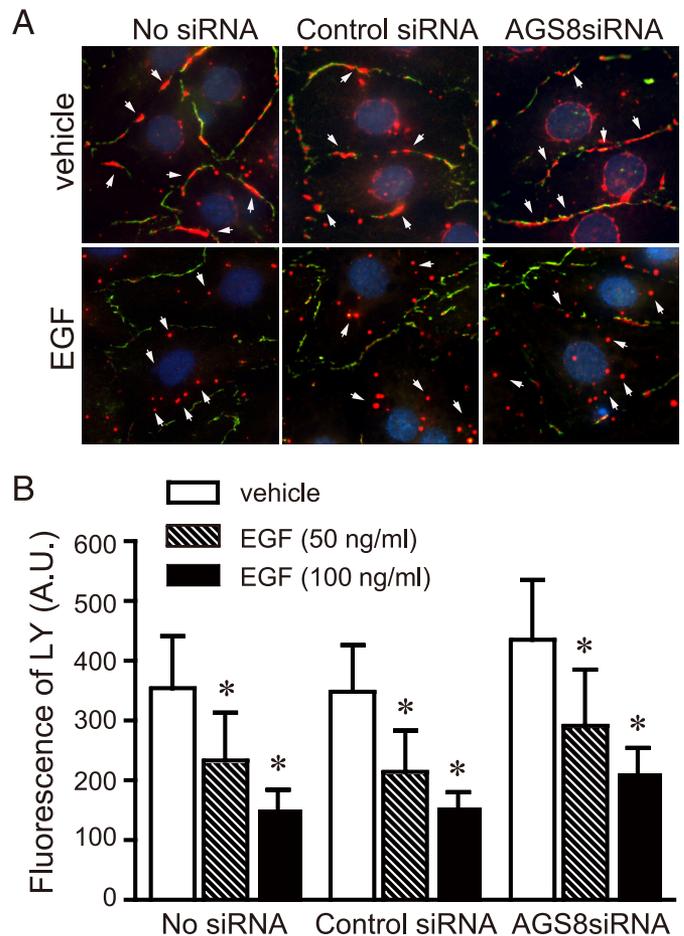
FIGURE 7. Influence of AGS8 on EGF-induced internalization of CX43 and change of permeability. *A*, an effect of AGS8siRNA on internalization of CX43. Cardiomyocytes were stimulated by 100 ng/ml EGF for 30 min 48 h after (without or with) transfection of universal negative siRNA control (Control siRNA) or AGS8siRNA2 (AGS8siRNA). Cells were immediately fixed and subjected to immunofluorescence stain for total CX43 as described under "Experimental Procedures." The figures demonstrated the triple stain of CX43 (*red*, *arrow*), N-cadherin (*green*), and nuclei (DAPI, *blue*). The data are representative of four independent experiments with similar results. *B*, uptake of fluorescence dye, LY, by the cardiomyocytes. The fluorescence of LY was evaluated by microscopy as described under "Experimental Procedures." The fluorescence of LY was quantified by the intensity of fluorescence of 10 randomly selected fields (10 × 20). *, $p < 0.05$ in one-way ANOVA. No statistical significance was observed among groups in two-way ANOVA. $n = 4$ from four independent experiments.

tribution and CX43 permeability before and during hypoxic stress.

AGS8 Stimulated Phosphorylation of CX43 in a $G\beta\gamma$-dependent Manner—The effect of AGS8 on CX43 phosphorylation and the involvement of $G\beta\gamma$ were determined in transiently transfected COS7 cells (Fig. 5, *A* and *B*). The expression of $G\beta\gamma$ or AGS8 alone did not influence the phosphorylation level of CX43. However, CX43 phosphorylation was significantly increased when cells were simultaneously transfected with AGS8 and $G\beta\gamma$. AGS8-$G\beta\gamma$ stimulated phosphorylation of serine 368 as well as serine 262 on CX43, indicating AGS8 and $G\beta\gamma$ regulated multiple phosphorylation sites of CX43. Furthermore, AGS8-C also stimulated phosphorylation of CX43 in the presence of $G\beta\gamma$, suggesting the functional importance of the C-terminal region of AGS8 and $G\beta\gamma$ input for CX43 phosphorylation. Because the level of phosphorylated CX43 was higher
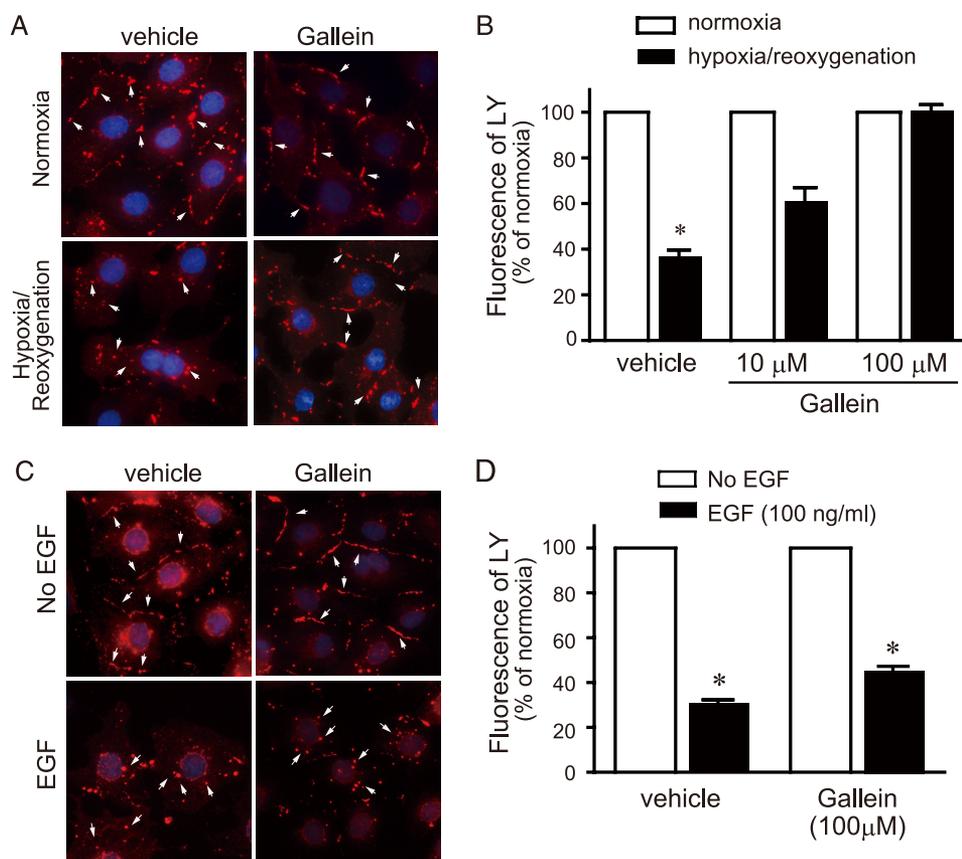
FIGURE 8. **Effect of Gallein on internalization and change of permeability of CX43 induced by hypoxia or EGF.** *A*, an effect of Gallein on internalization of CX 43. Cardiomyocytes were exposed 3 times to 30 min of hypoxia intermittant with 30 min of reoxygenation. After the third hypoxic period, cells were immediately fixed and subjected to immunofluorescence stain for total CX43 as described under "Experimental Procedures." The figures demonstrated the double stain of CX43 (*red, arrow*) and nuclei (DAPI, *blue*). The data are representative of four independent experiments with similar results. *B*, uptake of fluorescence dye, LY, by the cardiomyocytes. The fluorescence of LY was evaluated by microscopy as described under "Experimental Procedures." The fluorescence of LY was quantified by the intensity of fluorescence of 10 randomly selected fields (10×20). *, $p < 0.05$ in Kruskal-Wallis test followed by Dunn's multiple comparison post-hoc test. $n = 4$ from four independent experiments. *C*, an effect of Gallein on internalization of CX43. Cardiomyocytes were stimulated by 100 ng/ml EGF for 30 min, then cells were immediately fixed and subjected to immunofluorescence stain for total CX43. The figures demonstrated the double stain of CX43 (*red, arrow*) and nuclei (DAPI, *blue*). The data are representative of four independent experiments with similar results. *D*, uptake of fluorescence dye, LY, by cardiomyocytes. The fluorescence of LY was evaluated by microscopy as described under "Experimental Procedures." The fluorescence of LY was quantified by the intensity of fluorescence of 10 randomly selected fields (10×20). *, $p < 0.05$ *versus* control without EGF stimulation in Kruskal-Wallis test followed by Dunn's multiple comparison post-hoc test. $n = 4$ from four independent experiments.

when cells were co-transfected with AGS8 and $G\beta\gamma$ compared with cells transfected with $G\beta\gamma$ alone, these data suggest that AGS8 served as a scaffold to facilitate phosphorylation of CX43, rather than simply releasing free $G\beta\gamma$ from $G\alpha$ to activate $G\beta\gamma$ signaling.

The Requirement of AGS8 for Hypoxia-mediated Internalization of CX43—The phosphorylation of CX43 is associated with its internalization as well as turnover of the protein (30, 37, 38). An impact of AGS8siRNA on internalization of CX43 was determined in NCM following hypoxic stress. The large part of CX43 was observed in the cell surface, which was detected by N-cadherin (Fig. 6A). Exposure of cardiomyocytes to repetitive hypoxia induced internalization of CX43 in NCM with non-transfection as well as control siRNA (Fig. 6A). However, AGS8siRNA2 remarkably blocked the internalization of CX43 induced by repetitive hypoxia.

The hypoxia-induced internalization of CX43 was also associated with increased CX43 phosphorylation (30, 39). The immunofluorescence signals of phosphorylated CX43 were greatly enhanced in the presence of the proteasome inhibitor MG132, suggesting rapid degradation of phosphorylated CX43 as previously reported (30, 37). The majority of phosphorylated CX43 detected by serine 368 or serine 262 antibodies were observed in the cytoplasm following repetitive hypoxia in non-transfected NCMs as well as in the control siRNA group (Fig. 6, *B* and *C*). However, phosphorylated CX43 remained at the cell surface following knockdown of AGS8, suggesting a pivotal role of AGS8 in the internalization of CX43. A similar effect of AGS8 knockdown was also observed AGS8siRNA1 (supplemental Fig. S2*A*).

AGS8 Preserved Permeability of Small Molecule Flow Through CX43 Following Repetitive Hypoxia—The loss of hemichannel CX43 from the cell surface decreases influx and efflux of small molecules through CX43. AGS8-mediated regulation of CX43 may influence the permeability of small molecules involved in the fate of NCM under hypoxia. To address this issue, we examined the flux of dye through CX43 before and during hypoxic stress. Lucifer Yellow (LY) in the culture medium was incorporated into NCMs in a time-dependent manner.[6] Repetitive hypoxia decreased the accumulation of LY to $27.4 \pm 4.9\%$ ($p < 0.05$) in the non-transfected NCM or $34.1 \pm 10.6\%$ ($p < 0.05$) in control siRNA-transfected NCM compared with normoxia groups, respectively (Fig. 6*D*). However, interestingly, the permeability of CX43 was maintained in the NCM transfected with AGS8siRNA ($93.1 \pm 6.9\%$ *versus* normoxia, no statistical significance). This observation was consistent with immunofluorescence studies in which CX43 remained at the cell surface following repetitive hypoxia by knockdown of AGS8 (Fig. 6, *A–C*).

AGS8 was not Involved in Receptor-mediated Internalization of CX43—We next investigated if AGS8 regulated CX43 as a part of adaptive program of NCM in response to "hypoxic stress" or AGS8 is merely involved in the "general pathway" of

---

[6] Q. Jiao, and M. Sato, unpublished observations.

internalization of CX43. To address this issue, the effect of AGS8siRNA2 on receptor-mediated internalization of CX43 was examined. EGF stimulated phosphorylation of CX43 via the mitogen-activated protein kinase pathway that led to internalization of CX43 (37). EGF induced internalization of CX43 in non-transfected NCMs as well as control siRNA-transfected NCMs (Fig. 7*A*). In contrast to the effect of AGS8 knockdown on hypoxia-mediated internalization of CX43, AGS8siRNA did not alter EGF-mediated internalization of CX43. A similar result was observed with AGS8siRNA1 (supplemental Fig. S2*B*).

The accumulation of LY inside the cells is consistent with the influence of EGF on CX43 internalization. EGF decreased the permeability of CX43 in a dose-dependent manner, reflecting loss of CX43 at the cell surface (Fig. 7*B*). The permeability of CX43 was decreased in all of the groups to a similar extent. These observations were in contrast with the impact of AGS8siRNA in repetitive hypoxia, suggesting the AGS8-mediated signal was activated under hypoxic stress.

The Involvement of the Gβγ Signal in the Internalization of CX43—AGS8 was identified as a receptor-independent Gβγ signal regulator induced in the ischemic myocardium. AGS8 formed a scaffold with CX43/Gβγ in cells (Figs. 3 and 4), and stimulated phosphorylation of CX43 in a Gβγ-dependent manner (Fig. 5), suggesting that activation of the Gβγ signal is involved in the regulation of CX43. Thus, we examined the change of internalization and permeability of CX43 following treatment with the Gβγ signal inhibitor, Gallein, which occupied a "common" interaction surface of Gβγ and inhibited its interaction with Gβγ-regulated proteins (40).

Interestingly, Gallein blocked internalization of CX43 (Fig. 8*A*) and maintained LY uptake under repetitive hypoxia in a dose-dependent manner (Fig. 8*B*). Thus, Gallein mimicked the effect of AGS8siRNA in the regulation of CX43 upon hypoxic stress. Next, the effect of Gallein on EGF-mediated internalization of CX43 was further investigated. As observed with AGS8siRNA, Gallein did not block EGF-mediated internalization of CX43 nor block the decrease of LY uptake following EGF treatment, suggesting AGS8siRNA and Gβγ signal inhibitor had comparable effects on the regulation of CX43 in NCM (Fig. 8, *C* and *D*).

DISCUSSION

Here, we demonstrated the requirement of AGS8 for hypoxia-mediated apoptosis of cardiomyocytes. Interestingly, knockdown of an accessory protein for heterotrimeric G-proteins had a remarkable effect on survival of cardiomyocytes under hypoxic stress. The observations suggested the pivotal role of AGS8 in hypoxia-mediated cell death and the potential as a therapeutic target in selected pathologies. AGS8 altered the sensitivity of cardiomyocytes to hypoxic stress rather than constitutively activating the apoptotic pathway, since proapoptotic effects of AGS8 were not observed in cells cultured under normoxia. Subsequent experiments indicated that this reorganization was associated with internalization of CX43 as well as an associated reduction in permeability of small molecules (Fig. 9). We demonstrated that the ischemia-inducible G protein regulator, AGS8 altered survival of cardiomyocyte under hypoxia,
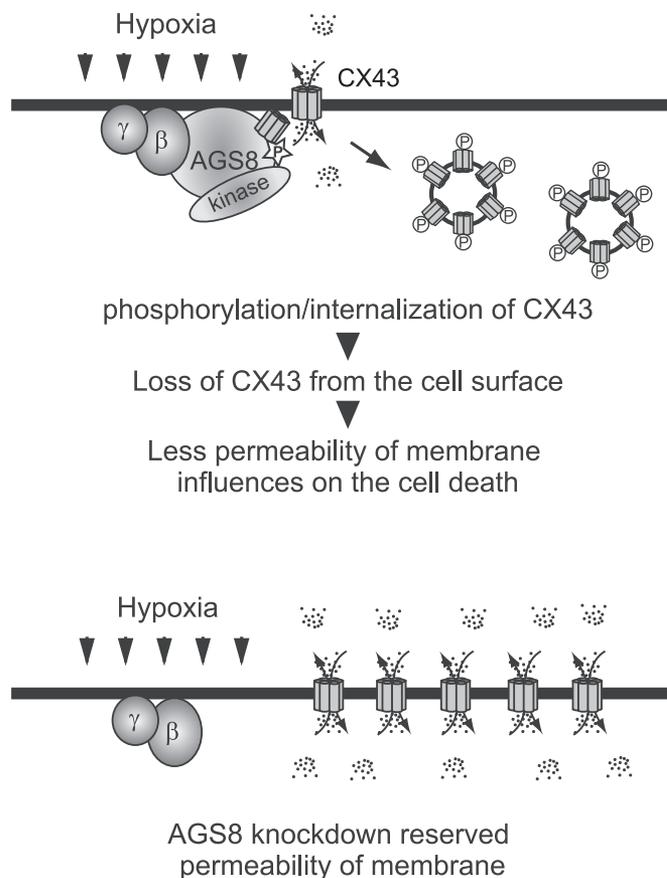
FIGURE 9. Schematic diagram indicating roles of AGS8 in regulation of connexin 43 in cardiomyocytes. *Upper panel*, AGS8 elicits phosphorylation of CX43 by serving as scaffold including CX43, Gβγ, and kinases. Phosphorylated CX43 leads to internalization of CX43 and decrease of channels in the plasma membrane. The decreased permeability of small molecule flow through CX43 influences apoptotic cell death under hypoxic stress. *Lower panel*, CX43 are not down-regulated following AGS8 knockdown by siRNA. The permeability of CX43 is maintained under hypoxic stress that may contribute to survival of cells.

which was associated with Gβγ-mediated regulation of CX43. Such activation of inherent programs involving a G protein regulator are particularly interesting for understanding the mechanism of cardiovascular disease.

Our data indicated that activation of Gβγ signaling was required for the hypoxia-induced CX43 internalization. The significant correlation of AGS8 with Gβγ suggested that AGS8 activated Gβγ pathway in response to hypoxic stress. The Gβγ regulator AGS8 formed a scaffold with CX43/Gβγ in cells and stimulated phosphorylation of CX43 with Gβγ (Figs. 3–5). Both AGSsiRNA and Gβγ signal inhibitor Gallein blocked the hypoxia-induced internalization of CX43 but not receptor-mediated internalization. AGS8 promoted Gβγ signal in cells as we demonstrated (8). These data suggest that AGS8 is involved in the activation of Gβγ signaling as a part of an adaptive program of NCM in the face of hypoxia that leads CX43 to internalization.

Ischemic injury of the myocardium is caused by the activation of multiple cascades initiating intracellular ionic and chemical changes that lead to cell death (21, 23). The channel protein CX43 is clearly involved in the apoptotic process by regulating the permeability of small molecules including aden-

osine 5′-triphosphate, adenosine diphosphate, adenosine, cAMP, inositol-1,4,5-trisphosphate, glutamate, and glutathione (26–29, 33). AGS8 reorganized cellular environments to be sensitive to hypoxic stress, at least in part, by controlling permeability of such molecules flowed through CX43. Functions of connexins are influenced by their phosphorylation and subcellular localization as well as protein turnover (36–38). Each step of regulation affects the fate of cells depending on the type of stress experienced by the cells (27, 35, 39, 41). In response to ischemia/hypoxia, AGS8 apparently coordinates the generation of a scaffold that includes CX43, $G\beta\gamma$ and possibly kinases that initiates CX43 phosphorylation leading to closure, internalization, and degradation of CX43 (27, 30, 36–38). Such a regulatory mechanism may play a critical role in the survival of cardiomyocytes under particular conditions. In contrast to our observations demonstrating the association of hypoxia-induced apoptosis with dynamic regulation of CX43, the reduction of CX43 itself did not show a significant effect on myocardial infarction in the heterozygous deletion mice (CX43$^{+/-}$) (35, 42), suggesting different adaptation mechanisms in the two challenges.

The adaptation program of cardiomyocytes to ischemia/hypoxia included the unexpected regulation of G-proteins and CX43 by AGS8. It would be important to validate the role of AGS8 and its association with CX43 in multiple systems including adult ventricular cardiomyocytes as well as a whole body model under various types of stress. Although the additional proteins involved in the phosphorylation as well as internalization of CX43 has yet to be determined, an investigation into the disruption of the AGS8 cascade may shed light on an approach for protection against cardiac ischemic injury.

REFERENCES

1. Birnbaumer, L. (2007) *Biochim. Biophys. Acta* **1768,** 772–793
2. Smrcka, A. V. (2008) *Cell Mol. Life Sci.* **65,** 2191–2214
3. Oldham, W. M., and Hamm, H. E. (2006) *Q. Rev. Biophys.* **39,** 117–166
4. Sato, M., Blumer, J. B., Simon, V., and Lanier, S. M. (2006) *Annu. Rev. Pharmacol. Toxicol.* **46,** 151–187
5. Cismowski, M. J. (2006) *Semin Cell Dev. Biol.* **17,** 334–344
6. Blumer, J. B., Smrcka, A. V., and Lanier, S. M. (2007) *Pharmacol. Ther.* **113,** 488–506
7. Sato, M., Gettys, T. W., and Lanier, S. M. (2004) *J. Biol. Chem.* **279,** 13375–13382
8. Sato, M., Cismowski, M. J., Toyota, E., Smrcka, A. V., Lucchesi, P. A., Chilian, W. M., and Lanier, S. M. (2006) *Proc. Natl. Acad. Sci. U.S.A.* **103,** 797–802
9. Blumer, J. B., Lord, K., Saunders, T. L., Pacchioni, A., Black, C., Lazartigues, E., Varner, K. J., Gettys, T. W., and Lanier, S. M. (2008) *Endocrinology* **149,** 3842–3849
10. Sato, M., and Ishikawa, Y. (2009) *Pathophysiology*, 10.1016/j.pathophys.2009.03.011
11. Hendriks-Balk, M. C., Peters, S. L., Michel, M. C., and Alewijnse, A. E. (2008) *Eur. J. Pharmacol.* **585,** 278–291
12. Heximer, S. P., Srinivasa, S. P., Bernstein, L. S., Bernard, J. L., Linder, M. E., Hepler, J. R., and Blumer, K. J. (1999) *J. Biol. Chem.* **274,** 34253–34259
13. Rogers, J. H., Tamirisa, P., Kovacs, A., Weinheimer, C., Courtois, M., Blumer, K. J., Kelly, D. P., and Muslin, A. J. (1999) *J. Clin. Invest.* **104,** 567–576
14. Yuan, C., Sato, M., Lanier, S. M., and Smrcka, A. V. (2007) *J. Biol. Chem.* **282,** 19938–19947
15. Yogo, K., Ogawa, T., Akiyama, M., Ishida, N., and Takeya, T. (2002) *FEBS Lett.* **531,** 132–136
16. Li, J., Niu, X. L., and Madamanchi, N. R. (2008) *J. Biol. Chem.* **283,** 34260–34272
17. Sato, M., Ribas, C., Hildebrandt, J. D., and Lanier, S. M. (1996) *J. Biol. Chem.* **271,** 30052–30060
18. Toyota, E., Warltier, D. C., Brock, T., Ritman, E., Kolz, C., O'Malley, P., Rocic, P., Focardi, M., and Chilian, W. M. (2005) *Circulation* **112,** 2108–2113
19. Hausenloy, D. J., and Yellon, D. M. (2007) *Pharmacol. Ther.* **116,** 173–191
20. Webster, K. A. (2007) *Trends Pharmacol. Sci.* **28,** 492–499
21. Yellon, D. M., and Hausenloy, D. J. (2007) *N. Engl. J. Med.* **357,** 1121–1135
22. Cook, S. A., Sugden, P. H., and Clerk, A. (1999) *Circ. Res.* **85,** 940–949
23. Bishopric, N. H., Andreka, P., Slepak, T., and Webster, K. A. (2001) *Curr. Opin. Pharmacol.* **1,** 141–150
24. Saffitz, J. E. (2005) *Ann. N.Y. Acad. Sci.* **1047,** 336–344
25. Lampe, P. D., Cooper, C. D., King, T. J., and Burt, J. M. (2006) *J. Cell Sci.* **119,** 3435–3442
26. Solan, J. L., Marquez-Rosado, L., Sorgen, P. L., Thornton, P. J., Gafken, P. R., and Lampe, P. D. (2007) *J. Cell Biol.* **179,** 1301–1309
27. Bao, X., Lee, S. C., Reuss, L., and Altenberg, G. A. (2007) *Proc. Natl. Acad. Sci. U.S.A.* **104,** 4919–4924
28. Rodríguez-Sinovas, A., Cabestrero, A., López, D., Torre, I., Morente, M., Abellán, A., Miró, E., Ruiz-Meana, M., and García-Dorado, D. (2007) *Prog. Biophys. Mol. Biol.* **94,** 219–232
29. Harris, A. L. (2007) *Prog. Biophys. Mol. Biol.* **94,** 120–143
30. Laird, D. W. (2005) *Biochim. Biophys. Acta* **1711,** 172–182
31. Ruiz-Meana, M., Rodríguez-Sinovas, A., Cabestrero, A., Boengler, K., Heusch, G., and Garcia-Dorado, D. (2008) *Cardiovasc. Res.* **77,** 325–333
32. Rodriguez-Sinovas, A., Boengler, K., Cabestrero, A., Gres, P., Morente, M., Ruiz-Meana, M., Konietzka, I., Miró, E., Totzeck, A., Heusch, G., Schulz, R., and Garcia-Dorado, D. (2006) *Circ. Res.* **99,** 93–101
33. Shintani-Ishida, K., Uemura, K., and Yoshida, K. (2007) *Am. J. Physiol. Heart Circ. Physiol.* **293,** H1714–H1720
34. Schulz, R., Gres, P., Skyschally, A., Duschin, A., Belosjorow, S., Konietzka, I., and Heusch, G. (2003) *Faseb J.* **17,** 1355–1357
35. Heinzel, F. R., Luo, Y., Li, X., Boengler, K., Buechert, A., García-Dorado, D., Di Lisa, F., Schulz, R., and Heusch, G. (2005) *Circ. Res.* **97,** 583–586
36. Ek-Vitorin, J. F., King, T. J., Heyman, N. S., Lampe, P. D., and Burt, J. M. (2006) *Circ. Res.* **98,** 1498–1505
37. Leithe, E., and Rivedal, E. (2004) *J. Cell Sci.* **117,** 1211–1220
38. Fernandes, R., Girão, H., and Pereira, P. (2004) *J. Biol. Chem.* **279,** 27219–27224
39. Turner, M. S., Haywood, G. A., Andreka, P., You, L., Martin, P. E., Evans, W. H., Webster, K. A., and Bishopric, N. H. (2004) *Circ. Res.* **95,** 726–733
40. Lehmann, D. M., Seneviratne, A. M., and Smrcka, A. V. (2008) *Mol. Pharmacol.* **73,** 410–418
41. Retamal, M. A., Schalper, K. A., Shoji, K. F., Bennett, M. V., and Sáez, J. C. (2007) *Proc. Natl. Acad. Sci. U.S.A.* **104,** 8322–8327
42. Schwanke, U., Konietzka, I., Duschin, A., Li, X., Schulz, R., and Heusch, G. (2002) *Am. J. Physiol. Heart Circ. Physiol.* **283,** H1740–H1742